Super absorption and efficient absorption of light by spherical nanoparticles

Konstantin Ladutenko*
ITMO University, 49 Kronverskii Ave., St. Petersburg 197101, Russian Federation
and
Ioffe Physical-Technical Institute of the Russian Academy of Sciences, 26 Polytekhnicheskaya Str., St. Petersburg 194021, Russian Federation

Ovidio Peña-Rodríguez
Instituto de Fusión Nuclear, Universidad Politécnica de Madrid, José Gutiérrez Abascal 2, E-28006 Madrid, Spain

Ali Mirzaei, Andrey Miroshnichenko, and Ilya Shadrivov
Nonlinear Physics Centre, Research School of Physics and Engineering, The Australian National University, 59 Mills Rd, Acton, ACT, 2601, Australia
(Dated: June 16, 2015)

Spherical subwavelength nanoparticles have a fundamental limit as to how much light they can absorb. This limit is based on the assumption that only one mode is excited in the nanoparticle. Using stochastic optimization algorithm, we design multi-layer nanoparticles, in which we can make several resonant modes overlap at the same frequency, thus significantly beating the theoretical limit of absorption, and we call this super-absorption. We further introduce the efficiency of the absorption for a nanoparticle, which is absorption normalized by the physical size of the particle, and show that efficient absorbers are not always operating in super-absorbing regime.

PACS numbers: 41.20.Jb 42.25.Bs 02.60.Pn 02.70.-c

Mie theory [1], which is over 100 years old now, describes interaction of electromagnetic waves with spherical particles. Mie solution is still of great interest these days [2–8], since it is one of the primary tools for analyzing wave scattering by spherical objects. Further development of the Mie theory [9, 10] made it possible to apply study the multilayered spherical particles [11, 12]. Such particles have various applications in cancer treatment [13, 14] and medical diagnostics [15], cloaking [16–18] and plasmonic [19, 20] devices, study on thermal properties of insulating material [21], as well as for improving solar cells performance [22, 23], and so on.

The scattering properties of multilayer cylinders and spheres was studied in great detail by Fan et al. [24, 25]. In these works authors introduced the concept of a super scattering, when the scattering cross-section of a multilayer particle exceeds that of a homogeneous particle of the same size in the so-called single-channel limit. The super scattering appears when we design a multilayer structure so that several modes become nearly degenerate, i.e. their resonance frequencies coincide or get close to each other. In a homogeneous particle, the resonances appear at different frequencies, and there is no design freedom for a fixed geometry of the structure to make these resonances overlap, and this limits the achievable scattering cross-section.

Similar fundamental limitations exist for the absorbing properties of sub-wavelength nanoparticles. Tribelsky [26] has derived a theoretical limit of a maximum absorption cross-section (ACS) value for a single channel, i.e., when only one mode of the sphere is excited. As a result the absorption coefficients $\tilde{a}_n = \mathrm{Re}\{a_n\} - |a_n|^2$ and $\tilde{b}_n = \mathrm{Re}\{b_n\} - |b_n|^2$ become limited by $1/4$, here a_n and b_n are scattering coefficient as defined in Mie theory [27].

To overcome these limitations, we employ similar approach for enhancing absorption cross-section [25]. In particular, we propose to use the multi-layer structures, and by means of genetic algorithm we optimize the ACS of these particles. We analyze the absorption cross-section of these particles, and present the super-absorption regime. We further introduce the absorption efficiency, which is the ACS normalized to the geometric cross-section of the particles. Here we show that there is a strong counter-play between the increased absorption for larger particles vs size for smaller particles, and quite remarkably we find that the most *efficient* absorption can be achieved in a single channel limit for small particles.

We should note a recent work of Grigoriev et al. [36] with expressions for ideal absorber; however, they considered only a dipole approximation, the final value for our range of particle sizes is very close to the dipole limit predicted with Tribelsky [26]. This way super-absorption designs are out of scope from the Grigoriev ideal case; moreover, Grigoriev also provide an equation to desing a core-shell structure from predefined materials. However, in case of material parameters that we used for Si and Ag and size parameter from our best design, Grigoriev's equation gives a complex value for relative share of two layers, which is not suitable for most of the simulation

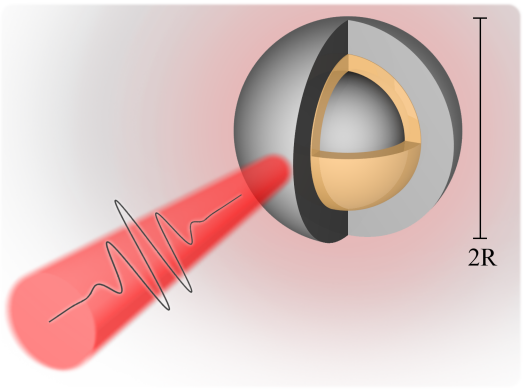

Figure 1. Shematic view of the simulated $Si/Ag/Si$ particle.

software or experiment.

We start our analyses by considering the triple layered $Si/Ag/Si$ spherical particle illuminated with a plane wave (Fig. 1). In what follows we describe the materials using experimentally measured parameters from the Ref. [28]. To optimize the thickness of each layer we implemented [29] an adaptive differential evolution algorithm [30], which is called JADE [31]. The technical details of the optimization algorithm are published previously in Ref. [18]. We perform Mie calculations using the Scattnlay [10, 32] software, whose results were verified with a number of other implementations of the Mie solutions and with a commercially available software such as CST Microwave studio [34] and Comsol Multiphysics [33].

It is obvious that in general, a bigger particle will have a bigger absorption cross-section, so sphere with the diameter of 1 cm will absorb more light than any sphere at the nanoscale. Therefore, we use absorption efficiency $Q_{\text{abs}} = C_{\text{abs}}/2\pi R^2$, where R is the outer radius of the particle and C_{abs} is the absorption cross-section. We maximize absorption efficiency at a fixed wavelength of incident light (we have chosen $\lambda = 500$ nm).

In order to study the dependence of the absorption efficiency on the outer particle size, we run optimization algorithm for different (fixed) particle outer size, and our optimization parameters are the radii of internal cores, whereas the target function is the absorption efficiency. We show the results of our genetic optimization algorithm in Fig. 2 (a). Dashed lines show theoretical absorption limit of a dipole ($n = 1$) and a quadrupole ($n = 2$) resonances [26], which are given as

$$Q^{(n)}_{\text{abs max}} = \frac{2n+1}{2q^2},$$

where the size parameter $q = 2\pi R/\lambda$, and n is an angular momentum of the mode. Following Ref. [25], where authors introduce super scattering for spherical particles, here we we introduce super-absorption, when the ACS

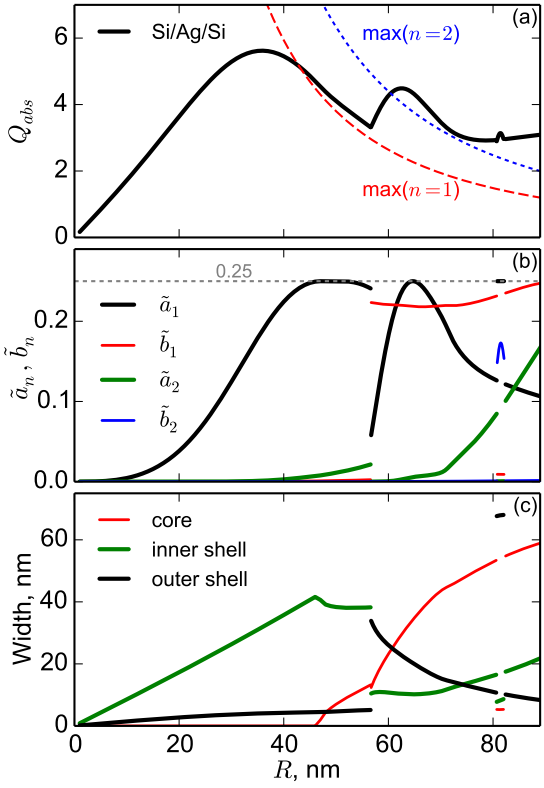

Figure 2. Results of the optimization of the absorption efficiency for the fixed wavelength of 500 nm. (a) Absorption efficiency with the best value achieved at the particle radius of 36 nm and Ag/Si design (zero sized core). Dashed lines show theoretical limits for the first channel and second channel absorption. Second and third peaks in the absorption efficiency curve exceed the theoretical limit for the second mode absorption at $R = 63$ nm and $R = 81$ nm. (b) Mie absorption coefficients for individual excited modes of the optimized structures. (c) Optimized layer thicknesses. For the total particle radius below 46 nm the optimizer converges to the two-layer structure, when core size vanishes, and the optimum design is a bi-layer Ag/Si particle.

is larger than the theoretical limit for absorption by the mode with highest excited angular momentum n. In our parameter space we have just modes up to the quadrupole excited ($n = 2$), and in order to get a super-absorption our efficiency should be higher than that of a quadrupole. We clearly see this super-absorption at $R > 60$ nm, in Fig. 2 (a).

In Fig. 2 (b) we present the values of Mie absorption coefficients for individual excited modes in the structure, while horizontal dashed line shows the theoretical limit (1/4) for each of them. $\tilde{a}_{1,2}$ are electric dipole and electric quadrupole, while $\tilde{b}_{1,2}$ are magnetic dipole and magnetic quadrupole. For small particles, as expected, the absorption is dominated by an electric dipole $\tilde{a}_1$. At $R > 56.6$ nm the optimization procedure finds that the designs with both electric and magnetic dipoles have larger ACS, than the structure with only the elec-

tric dipole excited. This is why the curves in Figs. 2 (b,c) experience the discontinuity. We also note that there is a very narrow range of particle sizes, between 80.7 nm and 82.1 nm, where our analyses finds that the design supporting electric dipole $\tilde{a}_1$ and magnetic quadrupole $\tilde{b}_2$, has larger ACS, and this explains two more discontinuities of the curves at the respective size values.

Fig. 2 (c) shows optimized sizes of the layers inside the multi-layer structure. It reveals quite a curious result, that the dipole branch (i.e. for particle radii below 56.6 nm) has two parts. For $R < 46$ nm the best absorber has just two layers, as the radius of the core of the three-layer structure vanishes, and the particle reduces to Ag/Si core-shell structure. At $R = 46$ dipole channel becomes practically undistinguishable from the theoretical limit (it becomes $\tilde{a}_1 > 0.249$). It appears that the optimizer introduced the inner Si layer in order to keep $\tilde{a}_1$ near the theoretical limit as the R increases. As a side effect, the quadrupole contribution $\tilde{a}_2$ appears, however, it does not help to reach super-absorption limit $n = 2$.

Remarkably, the absolute maximum absorption efficiency is not reached within the super-absorption regime. Figure 2 shows that the maximum efficiency is reached for small particle size, and the ACS is still well below the single channel limit. It appears that the Ag/Si core-shell nanoparticle, with the total radii of approximately 36 nm is the most efficient absorbing in the considered structure, which ACS reaching values over 5 times the physical cross-section area of the particle. From practical point of view it is quite important that the maximum can be reached in a bi-layer structure, instead of a triple-layer, and it should be easier and cheaper to produce.

To study spectral properties of the structures with large ACS which we obtained by the optimization, in Fig. 3 we plot three different cases for designs that correspond to local maxima of Q_{abs} shown in Fig. 2 (a). As expected, the design corresponding to the maximum absorption efficiency at $R = 36$ nm has a single electric dipole resonance centered at the target wavelength $\lambda = 500$ nm. Spectra of designs with maxima at $R = 63$ nm and $R = 81$ nm have a signature of the super absorption, i.e. there is an overlap of several resonances. We note that these structures have additional absorption resonances, but they are located far from the wavelength of interest.

A noticeable feature of Fig. 3 (c) is an almost flat top of the electric dipole resonance. We do not have any good explanation for this phenomena, however, we can suggest that it is due to coupling of the electric dipole $\tilde{a}_1$ with the magnetic quadrupole $\tilde{b}_2$. Whereas resonant responses of other desings originate from coupling of incident plane wave with the corresponding multipole, it is not the case for the design with $R = 81$ nm. Here, the particle is mostly composed from the Si outer shell, that give enough volume for $\tilde{b}_2$. Dipole response comes from the small inner part of the sphere and can not be

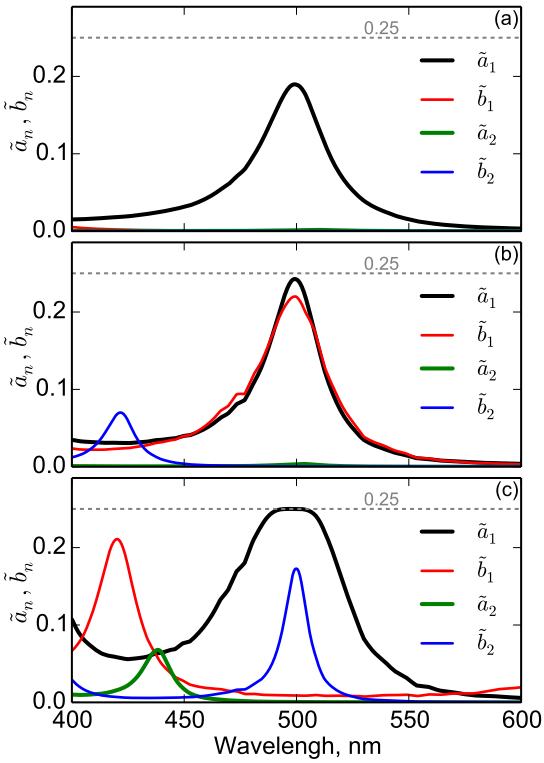

Figure 3. Spectra of Mie absorption coefficients of (a) efficient and (b-c)super absorption design.

directly exited with the incident wave. It takes the power from the surrounding $\tilde{b}_2$ mode and very soon it reaches the fundamental limit for absorption. This way we can observe a flat top for the $\tilde{a}_1$ response accompanied with a sigificat value of $\tilde{b}_2$. Our suggestion is indirectly proved by the reduced width of the $\tilde{b}_2$ resonance compared to other quadrupole responses.

Finally, we present distribution of the amplitude of the electric field in Fig. 4 for two designs: with the best efficiency at $R = 36$ nm and in a super-absorbing design with $R = 63$ nm. We also plot streamlines of the Poynting vector which characterize energy flow. For the effective design of the absorber, the power from a large cross-sectional area flows into the particle. In case of super-absorption regime, we observe power flow vortices, which make absorbtion more efficient as the electromagnetic energy propagates several times through the absorbing materials.

This way we conclude, that to design a good absorber it is not necessary to superpose several resonances. The explanation for the phenomena seems to be quite intuitive. Due to spatial structure of higher multipoles, namely presence of nodal points, they are not using efficiently the whole volume of the particle for the absorption. At the same time in 3D the increased absorption of higher multipoles should compete against quadratic growth of the geometrical cross-section. It is clearly not the point

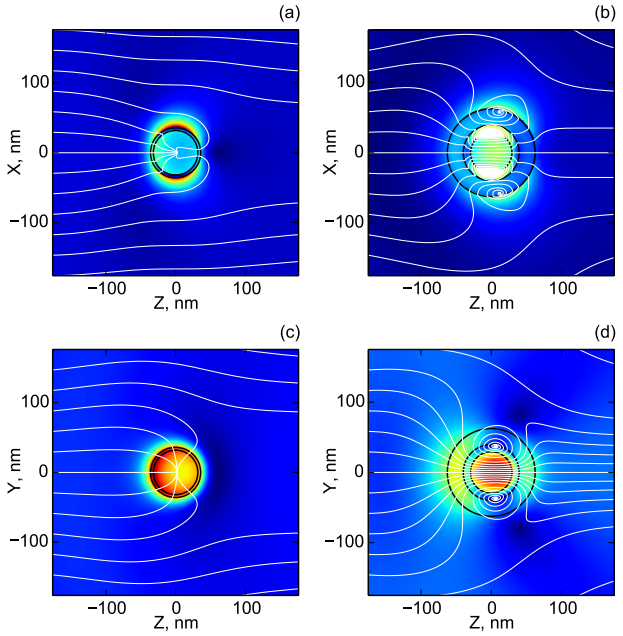

Figure 4. Amplitude of electric field for $R = 36$ nm (a,c) and "super" (b,d) designs in E-k (a-b) and H-k (c-d) planes.

for the case under consideration, the most efficient design has simply the smallest radius.

In conclusion, we find the effect of the super-absorption, when the absorption cross-section of the nanoparticle can exceed the theoretical limit for the absorption by the highest excited mode. This occur when several resonance modes of the structure overlap at the same frequency. We introduce efficiency of the absorption as an absorption cross-section divided by a geometric cross-section of the particle, and quite unexpectedly we find that the most efficient absorbers are smaller nanoparticles working in a single mode regime. We present their spectral characteristics and field structure.

It is interesting, that similar conclusion was made by Miller et al. [35] for extinction of arbitrary particles: small size with only dipole responce is preferable for geometric volume normalized efficiency.

TODO acknowledgments

* e-mail: fisik2000@mail.ru

[1] G. Mie, Annalen der Physik **330**, 377 (1908).
[2] H. Suzuki and I.-Y. S. Lee, International Journal of Physical Sciences **3**, 038 (2008).
[3] D. MacKowski, Springer Series in Optical Sciences **169**, 223 (2012).
[4] J. Lermé, The European Physical Journal D - Atomic, Molecular, Optical and Plasma Physics **10**, 265 (2000).
[5] H. Xu, Phys. Rev. B **72**, 073405 (2005).
[6] R. Li, X. Han, H. Jiang, and K. F. Ren, Appl. Opt. **45**, 1260 (2006).
[7] A. Gogoi, A. Choudhury, and G. Ahmed, Journal of Modern Optics **57**, 2192 (2010).
[8] M. A. Santiago-Cordoba, S. V. Boriskina, F. Vollmer, and M. C. Demirel, Applied Physics Letters **99**, 073701 (2011).
[9] W. Yang, Applied Optics **42**, 1710 (2003).
[10] O. Peña and U. Pal, Computer Physics Communications **180**, 2348 (2009).
[11] S. W. Sheehan, H. Noh, G. W. Brudvig, H. Cao, and C. A. Schmuttenmaer, The Journal of Physical Chemistry C **117**, 927 (2013).
[12] M. Selmke, M. Braun, and F. Cichos, ACS Nano **6**, 2741 (2012).
[13] J. Zhang, Journal of Physical Chemistry Letters **1**, 686 (2010).
[14] L. Hirsch, R. Stafford, J. Bankson, S. Sershen, B. Rivera, R. Price, J. Hazle, N. Halas, and J. West, Proceedings of the National Academy of Sciences of the United States of America **100**, 13549 (2003).
[15] L. R. Allain and T. Vo-Dinh, Analytica Chimica Acta **469**, 149 (2002).
[16] C.-W. Qiu, L. Hu, X. Xu, and Y. Feng, Phys. Rev. E **79**, 047602 (2009).
[17] X.Wang, F.Chen, and E. Semouchkina, AIP Advances **3**, 112111 (2013).
[18] K. Ladutenko, O. Peña Rodríguez, I. Melchakova, I. Yagupov, and P. Belov, Journal of Applied Physics **116**, 184508 (2014).
[19] J. Martin, J. Proust, D. Grard, and J. Plain, Optical Materials Express **3**, 954 (2013).
[20] A. Alu and N. Engheta, Phys.Rev.E **72**, 016623 (2005).
[21] T. Xie, Y.-L. He, and Z.-J. Hu, International Journal of Heat and Mass Transfer **58**, 540 (2013).
[22] Y. Kameya and K. Hanamura, Solar Energy **85**, 299 (2011).
[23] S. A. Mann, R. R. Grote, R. M. Osgood, and J. A. Schuller, Opt. Express **19**, 25729 (2011).
[24] Z. Ruan and S. Fan, Phys. Rev. Lett. **105**, 013901 (2010).
[25] Z. Ruan and S. Fan, Applied Physics Letters **98**, 043101 (2011).
[26] M. I. Tribelsky, EPL (Europhysics Letters) **94**, 14004 (2011).
[27] C. F. Bohren and D. Huffman, *Absorption and scattering of light by small particles*, Wiley science paperback series (Wiley, 1983).
[28] E. Palik, *Handbook of Optical Constants of Solids, Five-Volume Set: Handbook of Thermo-Optic Coefficients of Optical Materials with Applications* (Elsevier Science, 1997).
[29] `https://github.com/kostyfisik/jade`.
[30] R. Storn and K. Price, Journal of Global Optimization **11**, 341 (1997).
[31] J. Zhang and A. Sanderson, Evolutionary Computation, IEEE Transactions on **13**, 945 (2009).
[32] `https://github.com/ovidiopr/scattnlay`.
[33] `http://www.comsol.com/comsol-multiphysics`.
[34] `https://www.cst.com/Products/CSTMWS`.
[35] O. D. Miller, C. W. Hsu, M. T. H. Reid, W. Qiu, B. G. DeLacy, J. D. Joannopoulos, M. Soljačić, and S. G. Johnson, Phys. Rev. Lett. **112**, 123903 (2014).
[36] V. Grigoriev, N. Bonod, J. Wenger, and B. Stout, ACS Photonics **2**, 263 (2015), http://dx.doi.org/10.1021/ph500456w.